Article

# Chitosan-coated Mesoporous Silica Nanoparticle Treatment of Citrullus lanatus (Watermelon): Enhanced Fungal Disease Suppression and Modulated Expression of Stress-related Genes

Joseph T. Buchman, Wade Elmer, Chuanxin Ma, Kaitlin Landy, Jason C. White, and Christy L. Haynes

*ACS Sustainable Chem. Eng.*, **Just Accepted Manuscript** • DOI: 10.1021/acssuschemeng.9b04800 • Publication Date (Web): 11 Nov 2019

# Chitosan-coated Mesoporous Silica Nanoparticle Treatment of *Citrullus lanatus* (Watermelon): Enhanced Fungal Disease Suppression and Modulated Expression of Stress-related Genes

Joseph T. Buchman[§†], Wade H. Elmer[‡†*], Chuanxin Ma[∥], Kaitlin M. Landy[§], Jason C. White[∥], Christy L. Haynes[§*]

[†]These authors contributed equally to this work

[§]Department of Chemistry, University of Minnesota, 207 Pleasant St SE, Minneapolis, Minnesota 55455, United States

[∥]Department of Analytical Chemistry, The Connecticut Agricultural Experiment Station, 123 Huntington St, New Haven, Connecticut 06504, United States

[‡]Department of Plant Pathology and Ecology, The Connecticut Agricultural Experiment Station, 123 Huntington St, New Haven, Connecticut 06504, United States

**Corresponding authors**

*Prof. Christy Haynes, University of Minnesota, chaynes@umn.edu

*Dr. Wade H. Elmer, The Connecticut Agricultural Experiment Station, Wade.Elmer@ct.gov

**Abstract**

This work assesses the potential of mesoporous silica nanoparticles with or without a chitosan coating to suppress *Fusarium* wilt (*Fusarium oxysporum* f. sp. *niveum*) in watermelon (*Citrullus lanatus)* by virtue of dissolving to release silicic acid. Plant health was assessed by monitoring the total biomass and fruit production in both healthy and pathogen-infected plants up to 100 days after a single nanoparticle application (500 mg/L) was applied at the seedling stage. Both types of mesoporous silica nanoparticles enhanced the innate defense mechanisms of watermelon, with mesoporous silica nanoparticles (MSNs) and chitosan-coated mesoporous silica nanoparticles (CTS-MSNs) reducing disease severity by ~40% and ~27%, respectively, as measured by the area-under-the-disease-progress curve. Changes in gene expression measured several weeks after nanoparticle application demonstrated reduced expression of several stress-related genes after CTS-MSN and MSN treatments, indicating a reduced disease burden on the plant. Although treatment did not impact fruit production from diseased plants, a single application of chitosan-coated mesoporous silica nanoparticles at the seedling stage led to a 70% increase in the fruit yield of uninfected watermelon. Monitoring plant biomass revealed that MSNs and CTS-MSNs had no significant impact on the biomass reductions in diseased plants, likely because seedlings were treated and biomass was measured weeks later in the fully grown plants. These findings demonstrate the utility of a single application of mesoporous silica nanoparticles with or without a chitosan coating as a nano-enabled agricultural amendment, and current work is focused on optimizing the material synthesis and treatment regimens for maximum benefit.

**Keywords**

Nanoparticles, silica, chitosan, watermelon, *Fusarium* wilt, disease suppression, gene expression

## Introduction

Each year, approximately 20-40% of agricultural crops are lost to disease,[1] contributing significantly to global food insecurity. Soil-borne fungal pathogens, such as *Fusarium oxysporum* f. sp. *niveum* (FON),[2] infect the root systems of watermelon (*Citrullus lanatus*). After infecting the root system, the pathogen colonizes the vascular tissue, disrupting water transport within the plant, causing the symptomatic wilt, compromised growth, and potentially plant death.[3] For watermelon, *Fusarium* wilt is one of the major factors limiting global fruit production.[4] This resistant fungus is capable of surviving up to six years in soil without the presence of a host,[5] making it a particularly challenging pathogen to manage. According to the 2017 USDA Economic Research Service, over 45,000 ha of watermelons were grown in the US, producing over 40 million pounds.[6] The difficulty in managing *Fusarium* wilt on watermelon has increased for a number of reasons, including the discontinued use of methyl bromide due to toxicity concerns, more rapid cultivation times, and the use of more susceptible seedless watermelon varieties. Collectively, this has resulted in increased disease incidence and severity in an expanded area.[7–9] In response, greater focus on grafting, the use of cover crops, and more diverse biological control options have counteracted some of this spread, but there is still a significant need for novel management strategies.[7,10]

Although not essential, beneficial elements such as silicon play important roles in initiating the defense response of certain plants against diseases, insects, and stress.[11] While silicon accumulation is more commonly observed in monocotyledons, the family *Cucurbitaceae* are one of a few groups of dicotyledons known to accumulate significant amounts of silicon.[12] Silicon is acquired through roots as silicic acid and will often polymerize, forming silica phytoliths that fortify the plant's cell wall.[13] This enhanced barrier makes it more challenging for pathogens to penetrate and infect the plant tissues. Silicon is capable of stimulating plant metabolic defense mechanisms against disease by stimulating the activity of defense-related enzymes, such as polyphenoloxidase or chitinase, as well as inducing production of defense-related compounds like

flavonoids and phytoalexins, the details of which have been reviewed elsewhere.[14,15] While most studies have focused on root-absorbed silicon, a few reports have demonstrated that foliarly applied silica salts will reduce disease.[16] However, one limitation with silica applications is that the silicon supply to the plant must be continuous or the disease-suppressing effects will be reduced or non-existent.[17,18] One method with great potential for the efficient delivery of beneficial elements such as silicon is the use of slow-dissolving or controlled release nanoparticles for nutrient delivery.[19] Although many elements such as silicon and copper are not translocated basipetally, nanoscale forms of these nutrients have been shown to translocate from shoots to roots.[20] For copper, this more effective translocation has been associated with greater disease suppression in *Fusarium*-infected watermelon and tomato.[21,22] A formulation of silica called mesoporous silica was first reported in 1992,[23] and these materials are characterized by high surface areas and pore volumes, making them useful for many applications, potentially including slow release of silicic acid as the large surface area contacts the aqueous environment. The uptake and distribution of mesoporous silica nanoparticles in wheat, lupin, and *Arabidopsis* have been demonstrated.[24]

Other organic compounds such as chitosan have also been shown to be important in plant disease resistance. While there is some evidence of direct antifungal behavior from chitosan,[25] its greater effect is to initiate a signaling cascade within plants to bolster their natural defense mechanisms.[26,27] In fact, chitosan has been applied as a treatment for suppressing plant disease, the effects of which have been reviewed elsewhere.[28,29] For example, Bhaskara Reddy et al. demonstrated that *Fusarium graminearum* infection was controlled by treating wheat seeds with chitosan, which led to a >85% germination of seeds, and reduced the transmission of the fungus to the seedlings' primary roots.[30] Other benefits of a chitosan treatment include increased plant growth and overall fruit production,[31] as evident in the ~50% increase in fruit production from both chili and strawberry plants after chitosan application.[32,33] Due to their different pathways to

promote disease resistance, chitosan can be combined and co-treated with silica, and together, they have been shown to further enhance disease suppression.[34,35]

In this work, both mesoporous silica nanoparticles and chitosan-coated mesoporous silica nanoparticles were applied to *C. lanatus* to determine their ability to aid in defense against *Fusarium* wilt. Both silicon and chitosan are environmentally safe materials; silicon is the second most abundant element in Earth's crust, and chitosan is derived from chitin, the second most abundant renewable carbon source,[31] making use of these materials in agriculture quite sustainable. Mesoporous silica nanoparticles (MSNs) were employed because of their high surface area, which could facilitate faster degradation to monosilicic acid than nonporous silica, and for the ability to load various cargo (i.e. nutrients or pesticides) within the nanostructure for a synergistic delivery platform in future work.[36] MSNs and chitosan-coated MSNs (CTS-MSNs) were produced and characterized. A novel vacuum-infiltration technique was used to pre-treat watermelon seeds with MSNs and CTS-MSNs, investigating their effect on germination. Plants were also treated with MSNs or CTS-MSNs to assess the growth, biomass, and fruit yield in the presence of pathogenic *Fusarium* wilt. The silicon content in plant tissues was determined by inductively coupled plasma-mass spectrometry (ICP-MS), and quantitative reverse transcription polymerase chain reaction (RT-qPCR) was used to assess the expression of genes related to host defense. The findings show that a single application of these materials could significantly reduce disease progress in infected plants and in healthy plants, treatment with CTS-MSN significantly increased fruit production. Overall, this is the first example known to the authors that takes advantage of the combined impact of high surface area silica designed to release silicic acid and chitosan employed for nano-enabled agriculture.

## Experimental

### Materials

Tetraethylorthosilicate (TEOS), cetyltrimethylammonium bromide (CTAB), and chitosan (50-190 kDa) were obtained from Sigma-Aldrich (St. Louis, MO). Ammonium hydroxide ($NH_4OH$, 28-30% as $NH_3$) was purchased from Avantor Performance Materials (Center Valley, PA). Chlorotrimethyl silane was purchased from Fluka. Ammonium nitrate ($NH_4NO_3$) was acquired from Mallinckrodt (St. Louis, MO) and 2-[methoxy(polyethyleneoxy)$_{9\text{-}12}$propyl]-trimethoxysilane, tech 90 (PEG-silane, molecular weight 591-723 g/mol, 9-12 EO) was obtained from Gelest, Inc. (Morrisville, PA). Absolute ethanol was acquired from Pharmco-Aaper (Brookfield, CT). Ultrapure water (18.2 MΩ·cm resistivity) was purified from a Milli-Q Millipore water purification system (Billerica, MA). Watermelon seeds (*Citrullus lanatus* Thunb. cv Sugar Baby) were acquired from Harris Seed Co. (Rochester, NY) and the ProMix BX potting mix was purchased from Premier Hort Tech (Quakertown, PA). Peter's soluble 20-10-20 N-P-K fertilizer was obtained from R. J. Peter's Inc. (Allentown, PA).

### Synthesis of Mesoporous Silica Nanoparticles (MSNs)

MSNs were synthesized by adapting an established protocol.[37] Briefly, cetyltrimethylammonium bromide (0.29 g) was mixed with 0.256 M $NH_4OH$ (150 mL) with stirring (1 h, 300 rpm, 50 °C) [*caution: concentrated $NH_4OH$ is both toxic and corrosive!*] to form a surfactant template. Tetraethylorthosilicate (2.5 mL, 0.88 M) in ethanol was then added dropwise and stirred (1 h, 600 rpm, 50 °C), forming the silica structure around the CTAB micelles. Then, 2-[methoxy(polyethyleneoxy)$_{9\text{-}12}$propyl]-trimethoxysilane (450 µL) was added slowly and stirred (30 min, 600 rpm, 50 °C), followed by addition of chlorotrimethylsilane (68 µL) to modify the silica surface for dispersion stability. The beaker was immediately covered, and then the mixture was stirred (30 min, 600 rpm, 50 °C). Afterward, the cover was removed, and the MSNs were aged at 50 °C for ~20 hours.

The MSNs were purified with ultracentrifugation (30 min, 61,579×*g*) followed by resuspension in 6 g/L $NH_4NO_3$ (50 mL), which was refluxed for 1 h (300 rpm, 60 °C). After reflux, the suspension was ultracentrifuged for 20 min at 61,579×*g* (all subsequent ultracentrifugation steps used this duration and speed), resuspending the pellet in 95% ethanol. This suspension was again ultracentrifuged, resuspended in 6 g/L $NH_4NO_3$ (50 mL) and refluxed (1 h, 300 rpm, 60 °C). The suspension was then ultracentrifuged three more times, and resuspended in increasing ethanol concentrations (95%, 99%, 99% ethanol in water), and the final suspension was dried using a rotary evaporator to collect the powdered MSN product.

**Coating MSNs with Chitosan**

To coat the MSNs with chitosan, a procedure from Chen et al was adapted.[38] The chitosan coating adheres to the silica due to hydrogen bonding between the surface silanol groups of MSNs and amine groups on chitosan. A 0.6% w/v solution of chitosan was prepared in 10% v/v aqueous acetic acid. The pH was then adjusted to 6.0 using 1 M NaOH. Dried MSNs were added to the chitosan solution with magnetic stirring to prepare a 0.5% w/v suspension, typically with 100 mg of MSNs added to 20 mL chitosan solution. The suspension was then stirred at room temperature for 48 hours. Excess chitosan was removed via ultracentrifugation at 6842×*g* for 15 minutes. CTS-MSNs were then re-dispersed in water and collected by rotary evaporation. To characterize the chitosan coating, TEM imaging was used (described below), as well as determination of the hydrodynamic diameter and zeta potential. Changes in the porosity and surface area of the material were monitored with nitrogen physisorption, and the amount of chitosan coating was quantified using thermogravimetric analysis (TGA).

**Transmission Electron Microscopy**

To prepare the MSNs for imaging with TEM, the particles were diluted to 0.5 mg/mL in ethanol and sonicated for 10 min to ensure dispersity. Afterward, 200 mesh copper grids with

Formvar and carbon supports (Ted Pella, Inc., Redding, CA) were dipped in the suspension and allowed to air dry for 10 min. For the CTS-MSNs, they were first diluted to 0.5 mg/mL in water and sonicated for 10 min. Then, 3 μL of the suspensions were drop-cast onto TEM grids which were allowed to air dry overnight. Images were acquired using an FEI Tecnai T12 transmission electron microscope that was used at 120 kV operating voltage. To determine the size of the MSNs, the images were analyzed using ImageJ[39] to measure the diameter of at least 500 randomly selected nanoparticles.

**Hydrodynamic Diameter and Zeta Potential Measurements**

After synthesis of the MSNs and coating of CTS-MSNs, the nanoparticles were suspended in water at 500 mg/L. The nanoparticles were sonicated for 10 min to ensure that they were well-dispersed. The hydrodynamic diameters and ζ-potentials were then determined using a Brookhaven ZetaPALS instrument (Holtsville, NY).

**Nitrogen Physisorption**

Nitrogen physisorption was used to determine the surface area and pore volume of the MSNs and CTS-MSNs, and was utilized to confirm loading of chitosan onto the MSN surface. Approximately 15 mg of MSN were added (for CTS-MSNs, >60 mg were required) to the sample holder. The samples were degassed prior to analysis with a Micromeritics ASAP™ 2020 (Norcross, GA). The surface area and pore volume were determined using the BET method.

**Thermogravimetric Analysis**

Thermogravimetric analysis was used to assess the amount of chitosan on the MSN surface. MSNs and CTS-MSNs were first thoroughly dried using a rotary evaporator overnight. Then, ~10 mg of material were weighed onto an aluminum pan and placed onto a platinum tray. This was analyzed using a TA Instruments Q500 TGA (New Castle, DE) operated in a

temperature range from 25-550 °C (ramp rate: 10 °C/min) using 100 mL/min nitrogen gas (40 mL/min for balance, 60 mL/min for sample).

**Preparation of Millet Inoculum**

*F. oxysporum* f. sp. *niveum* (FON) isolate number CAESFON1 was isolated from infected watermelon seeds in 2011 and since then, monosporic cultures were stored at 4 °C. The FON inoculum was increased on sterile Japanese millet and ground in a mill using a previously published protocol.[40] The potting soil was infested with millet inoculum at 0.75 g/L potting soil prior to transplanting MSN-treated watermelon plants.

**Nanoparticle Application to *Citrullus lanatus***

To investigate the effect of nanoparticle application on the germination of watermelon seeds, the seeds were dosed with nanoparticles using a novel vacuum-infiltration technique that takes advantage of the air pockets in seed coats. One hundred watermelon seeds (*Citrullus lanatus* Thunb. cv Sugar Baby, Harris Seed Co., Rochester, NY) were placed in 30 mL suspensions of MSNs, CTS-MSNs, chitosan (250 and 500 mg/L each), or water. The solutions were moved to a desiccating chamber and were placed under vacuum using a vacuum pump for 10 min. The pressure was reduced to 0.6 Torr for 10 min, and then the vacuum was slowly released, which allows the seed coat air pockets to be backfilled with the nanoparticle-containing suspensions. Seeds were removed, drained, and immediately placed into 10 cm pots filled with FON-infested or non-infested potting soil (ProMix BX, Premier Hort Tech, Quakertown, PA). Approximately 20 seeds from each treatment were dried at 80 °C for 48 h, ground, and digested for ICP analysis described below to assess the silicon content. There were 10 replicate pots with five seeds per pot. Seedling emergence and growth was monitored for 14 days. To monitor the impact on plant growth and disease resistance, watermelon seeds were first germinated in ProMix BX potting mix. Three weeks later, they were fertilized with Peter's soluble 20-10-20 N-P-K

fertilizer (40 mL, R. J. Peter's Inc., Allentown, PA). One week after application of fertilizer, the watermelon plants were inverted and dipped for approximately 5 sec in 500 mg/L suspensions of MSNs, CTS-MSNs, chitosan, or bulk silica that had been amended with Regulaid nonionic surfactant (1 mL/L) (to enhance particle adhesion on the leaf surface), taking care to keep the roots unexposed. In the dipping process, each plant received approximately 1.5 mL of suspension (determined by looking at the volume of suspension in the graduated cylinder before and after dipping each plant). These suspensions had been probe sonicated for 2 min prior to this application to ensure particle dispersion. Plants were allowed to drain and dry upside down to minimize root contact with the nanoparticle amendments. Plants were then used in greenhouse and field trials.

For initial greenhouse growth, the plants were transplanted into pots containing either pathogen-free ProMix BX potting mix or potting mix with 0.75 g of millet inoculum per L of potting mix. These pots were kept in a greenhouse for the duration of the study. Select plants were transplanted to two locations (Griswold, CT and Hamden, CT) to monitor disease progress, plant growth, and fruit production under field conditions. Millet inoculum (~2 g) had been hand mixed into the planting holes (approximately 2 L volume of soil) for the *Fusarium*-infested treatment groups. There were twelve replicate microplots (one plant per microplot) in each treatment, with six microplots being exposed to the FON pathogen and six microplots being pathogen-free. The plants were arranged in the fields using a split plot randomized block. Weather information for these fields throughout the watermelon growing period can be found in the SI.

**Monitoring Seed Germination after Vacuum Infiltration of NPs**

To assess seed germination, the seeds that were vacuum-infiltrated with NPs as described above and were planted into pots containing pathogen-free potting mix or 0.75 g millet inoculum/L potting mix. Seeds began to emerge on day 4 and were counted daily for 2 weeks.

The cumulative seed germination was plotted and the area-under-the-seed-germination curve (AUSGC) was calculated using the trapezoid rule (Equation 1):

$$\boldsymbol{AUSGC = \sum[S_i + S_{(i+1)}]/2 \times (t_{(i+1)} - t_i)} \quad \textbf{(1)}$$

$\boldsymbol{S_i}$ is the number of seeds that had germinated at time, $\boldsymbol{t_i}$. These values were computed in the same manner as the area-under-the-disease-progress curve, described in Subsection 0.[41]

**Monitoring Disease Progress**

At 31, 61, and 95 days post-planting, the watermelon plants at Griswold, CT were assessed for the severity of *Fusarium* wilt, using a 1 to 5 scale (1 = no disease symptoms, 2 = slightly stunted, 3 = stunted and/or partially wilted, 4 = completely wilted, and 5 = dead). The cumulative severity ratings on the plants were plotted as a function of time, and disease progress is represented by the area-under-the-disease-progress curve (AUDPC); a higher AUDPC indicates more severe disease progress. The trapezoid rule was used to calculate the AUDPC (Equation 2), following a previously published procedure.[41]

$$\boldsymbol{AUDPC = \sum[Y_i + Y_{(i+1)}]/2 \times (t_{(i+1)} - t_i)} \quad \textbf{(2)}$$

In this equation, $Y_i$ is the disease severity rating at time, $t_i$.

In the greenhouse, plants were rated every 3-4 days beginning approximately 2 weeks days after the beginning of the study. After 5 weeks, the experiment was terminated and the root and shoot biomass were determined. Images of both pathogen-free and *Fusarium*-infected plants after several days can be seen in Figure S4.

**Gene Expression Changes**

**To monitor changes in the expression of select genes after NP treatment, total plant RNA was extracted from watermelon roots (~0.1 g) with a Sigma-Aldrich Spectrum Plant Total RNA kit (St. Louis, MO). This extraction was performed five weeks after the infected plants had been treated with nanoparticles so that the impact on gene expression could be investigated as a function of active disease and treatment. RNA was extracted**

**from the roots since that is the site of *Fusarium* infection in watermelon. The extracted RNA concentration was measured by a Thermo Scientific Nanodrop Lite Spectrophotometer (Wilmington, DE). A Qiagen QuantiTect Reverse Transcription kit (Velno, The Netherlands) was used for two-step reverse transcription on 1 µg of extracted RNA. RT-qPCR was then used to measure expression of several watermelon genes involved in plant stress and pathogen defense; in addition, several genes relevant in heavy metal regulation are included to facilitate comparison to other studies (**

Table 1). A Bio-Rad CFX96 Touch Real-Time PCR Detection System using the fluorescent intercalating dye, SYBR Green (Bio-Rad SsoAdvanced™ Universal SYBR® Green Supermix) was used. The polymerase chain reaction was run by maintaining the samples at 95 °C for 10 min to denature the DNA, and then 40 PCR cycles (95 °C for 15 sec then 60 °C for 60 sec), monitoring the SYBR Green fluorescence at the end of each cycle for DNA quantification. Relative expression of each gene was calculated by $2^{-\Delta\Delta Ct}$ method using Actin as the housekeeping gene.

**Table 1. List of genes used for gene expression analysis in this work. These genes are orthologs from *Arabidopsis thaliana* that are also found in *Citrullus lanatus*. *These are the NCBI accession numbers for these genes.**

| Target Gene | Gene Product | Function | Gene Identifiers |
|---|---|---|---|
| *CCH* | Copper chaperone | Involved in intracellular copper homeostasis regulation | Cla020497 |
| *COX11* | Cytochrome c oxidase assembly protein CtaG/COX11 family | Involved in copper delivery to the COX complex | Cla002392 |
| *PAO1* | Polyamine oxidase 1 | Polyamine catabolism | Cla015262 |
| *RAN1* | Heavy metal-exporting ATPase | ATP-dependent heavy metal transporter | Cla009875 |
| *CSD1* | Copper/zinc superoxide dismutase 1 | Alleviates superoxide radicals | Cla011299 |
| *PR1* | Pathogenesis-related protein 1 | Contributes to systemic acquired resistance in plants | Cla001623 |
| *PPO* | Polyphenol oxidase, chloroplastic-like | Oxidizes phenolic compounds | Cla019486 |
| *MDHA* | Malate dehydrogenase | Involved in central metabolism and redox homeostasis between organelle compartments | X17362* |
| *CYS* | Cysteine synthase | Synthesizes L-cysteine, a precursor for glutathione, which is involved in defending against stresses | D28777* |

**Nanoparticle Impact on Biomass**

After 65 and 100 days in the field, the fruit of watermelon plants were harvested, and the overall mass from each replicate plant was measured. At the end of the greenhouse experiment, the aboveground tissues and roots were separated, and their mass was measured and compared between treatments. Root systems were divided; half was dried for elemental analysis and half was frozen in liquid nitrogen and then moved to -80 °C until RT-qPCR could be performed. After obtaining the fresh weights of the tissues, they were then dried to constant weight in an oven at 50 °C.

**Silicon Content in Plant Tissues**

To determine whether silicon was accumulating in the treated plants, the aboveground tissues, roots, and fruit were dried to constant weight in a 50 °C oven. The dried tissues were then ground in a mill, and a 0.5 g portion was digested with 5 mL of concentrated nitric acid [*Caution: nitric acid is highly corrosive!*] for 45 min at 115 °C using a DigiPREP block digestion system (SCP Science, Champlain, NY). The samples were analyzed using an Agilent 7500ce inductively coupled plasma-mass spectrometer (Santa Clara, CA) to determine the silicon content.

**Statistical Analysis**

For comparisons of the different characterizations of uncoated and chitosan-coated MSNs, paired t-tests were used to determine statistical significance. Numerical representations of MSN and CTS-MSN characterization are denoted as mean±standard deviation. Statistical analysis of plant exposures was performed separately on healthy plants and *Fusarium*-infected plants using a one-way ANOVA with Tukey's multiple comparisons test ($p<0.05$) unless otherwise noted.

## Results and Discussion

### Characterization of Chitosan-coated MSNs

TEM was used to characterize the size of the mesoporous silica nanoparticles and their chitosan-coated counterparts. Three batches of MSNs were coated with chitosan, which had diameters of 36±7, 35±7, and 39±6 nm, as measured from TEM images. Representative TEM images of MSNs before and after coating can be seen in Figure 1. The mesoporous structure of MSNs is apparent in their TEM image, but after the addition of the chitosan coat, the mesopores are more obscured by the coating.

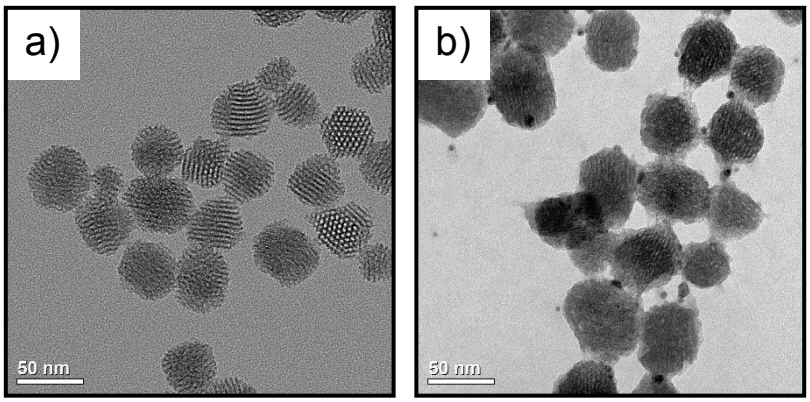


**Figure 1. Representative TEM images of a) bare mesoporous silica nanoparticles (MSNs) and b) MSNs after modification with chitosan (CTS-MSNs).**

The hydrodynamic diameters were measured before and after the chitosan coating, and the ζ-potential measurement was used to confirm the presence of the chitosan coat (Figure 2a, b). Results from the hydrodynamic diameter measurements suggest that the particles may be experiencing slight aggregation after being coated with chitosan, since the hydrodynamic diameter of the CTS-MSNs are approximately three times larger than that of the MSNs. Chitosan is a positively charged polysaccharide; therefore, evidence of its successful coating on MSNs is shown by the zeta potential measurements. Uncoated MSNs have a negative zeta potential (-39±3 mV), while chitosan-coated MSNs have a positive zeta potential (24±2 mV). This order of magnitude shift in the zeta potential of the nanoparticles before and after coating mirrors what has been observed previously.[42] Nitrogen physisorption was employed to observe the surface

area and pore volume change that arose from applying the chitosan coating (Figure 2c, d). A decrease in both surface area and pore volume indicate that the pores of the MSNs are being coated by or filled with the chitosan, decreasing the effective internal surface area of the nanoparticles as well as their overall pore volume. Moreover, the changes that are seen here are similar to those seen in the literature, although differences in the actual values are likely due to differences in the two systems, as the nanoparticles used by Chen and Zhu were also loaded with ibuprofen.[38] Infrared spectroscopy was also used to further characterize the success of the chitosan coating, details of which can be found in the SI. Thermogravimetric analysis was used to determine the mass contribution of chitosan to the chitosan-coated MSNs (Representative thermograms are in the SI). While the mass loss profiles collected here look similar to those in the literature, there was increased mass loss from our samples compared to those from Karaman, et al, as there was more chitosan present in our samples.[42] Based on evaluation of four replicate samples of CTS-MSNs, approximately 22±7% of the particle mass was from the polysaccharide coating.

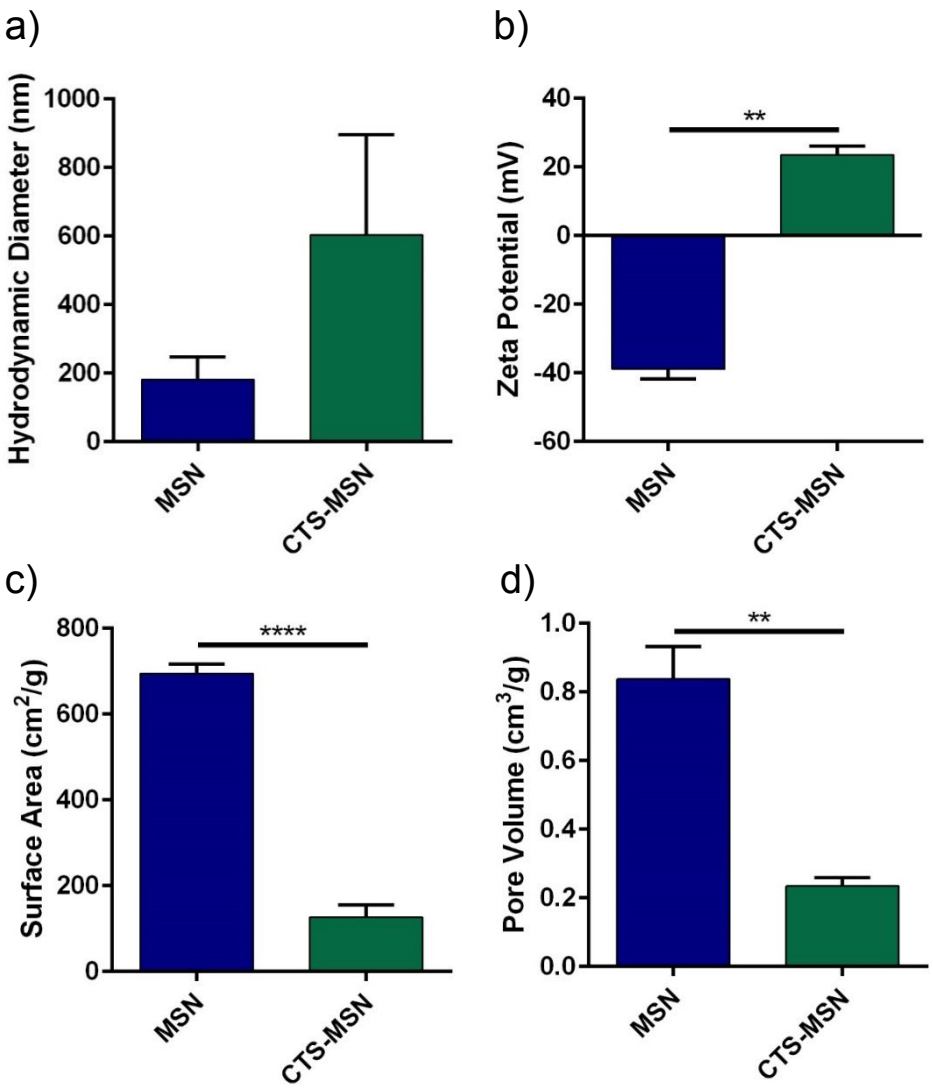


**Figure 2. The a) hydrodynamic diameters were determined before and after application of the chitosan coating. Evidence of successful chitosan coating can be seen in the b) zeta potential measurement, which shows that the bare MSNs had a negative surface charge and after coating, the surface charge was positive. A c) decrease in the surface area of the particles indicates that the pores are covered with chitosan, blocking the interior surface area of the particles, and d) the pore volume also decreased, again due to coverage of the pores by chitosan. The error bars represent the standard deviations from triplicate measurements, and paired t-tests were used to determine statistical significance between the uncoated and coated MSNs. **p<0.01, ****p<0.0001**

### Chitosan-coated MSNs Improve Germination of Watermelon Seeds

After exposing seeds to the various treatments using a novel vacuum-infiltration technique, the impact on seed germination percentage was assessed, and the AUSGC was

calculated. Representative images of seed germination after 11 days can be seen in Figure 3a. In seeds that were not infested with *F. oxysporum*, CTS-MSNs improved germination compared to the control at both concentrations tested (Figure 3b, c). Given that the initial germination percentage of seeds was 94%, we expect that although this treatment had slight increases in germination percentage, it caused the germination to occur more quickly in treated plants. We speculate that the improved germination from CTS-MSN treatment may be related to the chitosan content of the particles. This is corroborated by the fact that application of 250 mg/L of chitosan alone also increased germination. The mechanism by which chitosan can improve germination in seeds is not completely clear, however it is well known that it activates defense enzymes in plants and seeds.[30,43]

A separate study to confirm nanoparticle loading was done with ICP-MS of seeds that had been loaded with MSNs. This showed that seeds that were loaded with the 500 mg/L MSN suspension had significantly more silicon content (a 20% increase) than untreated seeds, and those that had been exposed with 250 mg/L MSN suspension had approximately 7% more silicon (Figure S5). This demonstrates that nanoparticle loading of the seeds was successful, and it is expected that loading was successful for all of the nanomaterials used in this study. Treatment with chitosan-free MSNs did lead to slightly increased germination, but this increase was not statistically significant, which further corroborates the fact that the additional silicon in the treated seeds is not responsible for the increased germination that was observed. In seeds planted in *Fusarium*-infested soil, germination was not affected by any of the treatments.

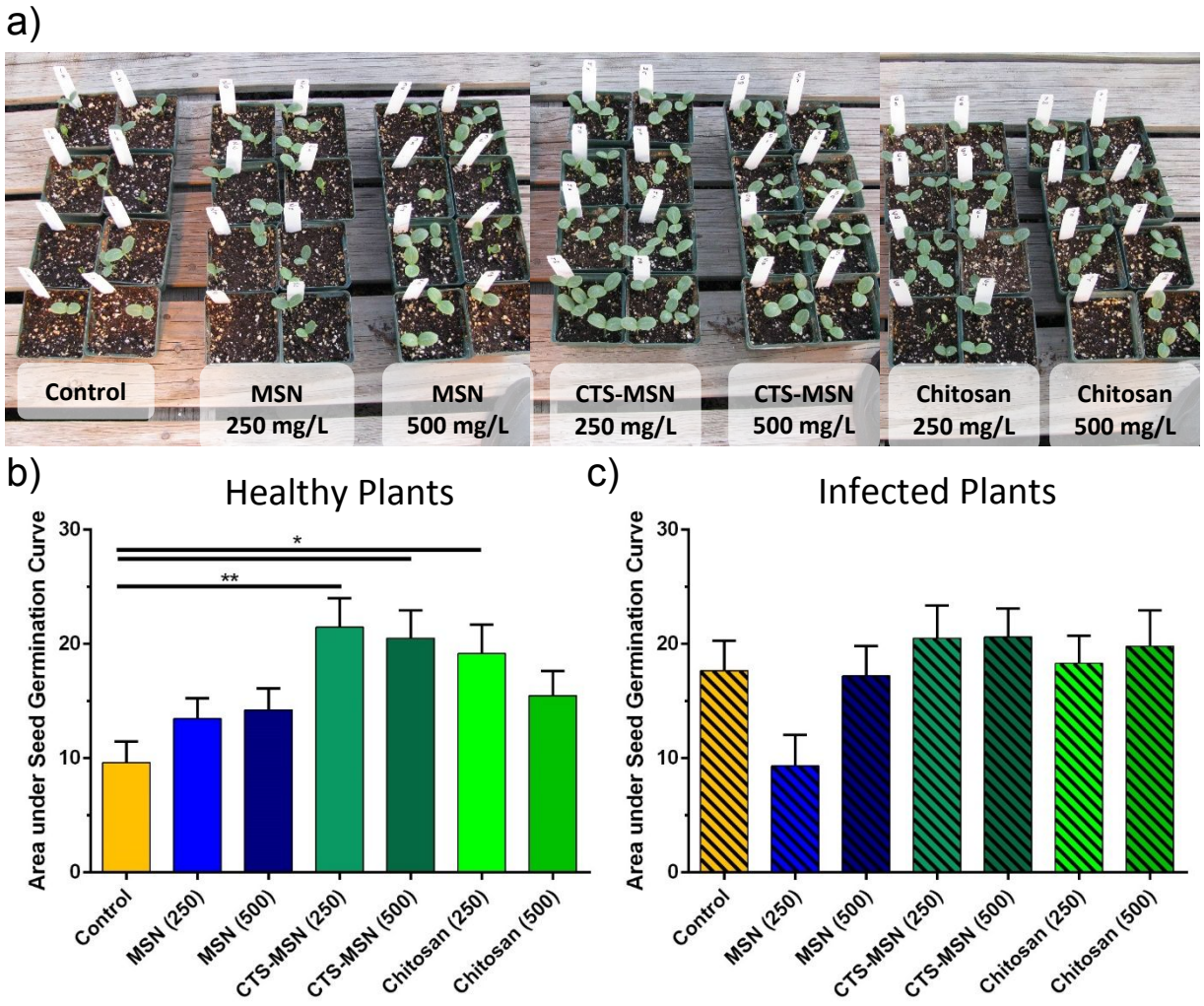


**Figure 3. a) Images showing the differences in germination after seeds were treated with NP-containing suspensions using a vacuum-infiltration technique. The area-under-the-seed-germination curve was evaluated after treatment: b) chitosan-coated MSNs improve the germination of seeds in healthy plants, but that c) germination was unaffected in seeds planted in *Fusarium*-infested soil. The error bars are the standard error of ten replicates. Statistical testing was performed using a one-way ANOVA with Dunnett's multiple comparisons test. *p<0.05, **p<0.01**

## Role in Disease Suppression

In the field experiments, the role of MSNs and CTS-MSNs in suppressing *Fusarium* wilt was evaluated by determining the AUDPC (Figure 4). Not surprisingly, in healthy plants, there was no change in the AUDPC with treatment and no symptoms of infection with *F. oxysporum*

were evident. However, with infected plants, treatment of the plants with both MSNs and CTS-MSNs resulted in significant disease suppression (disease progress was reduced by ~40% and 27% for MSN and CTS-MSN treatment, respectively) over the experiment. Since *F. oxysporum* is present in the roots and the nanoparticles are applied foliarly, the nanoparticles and pathogens should never be in direct contact here, and therefore there should be no direct toxicity between them. This indicates that the disease reduction observed here is due to the nanoparticles bolstering the natural defenses of *C. lanatus* to fight off the pathogen itself. Since both types of particles are exerting benefit, it is clear that the delivery of silica to the plant is critical to the observed disease suppression. For the CTS-MSNs, it is also possible that the presence of chitosan is helping to stimulate the defense response of the plants against *Fusarium* wilt. However, the lack of response in the MSN-free chitosan control suggests that association with the MSN is driving the observed activity. It should be noted that bulk silica treatment does not suppress *Fusarium* wilt, indicating the importance of the nanoscale size regime for the silica treatment to have an impact. Similar effects of these materials to different pathogen/plant systems have been observed,[34,35] corroborating the results obtained herein.

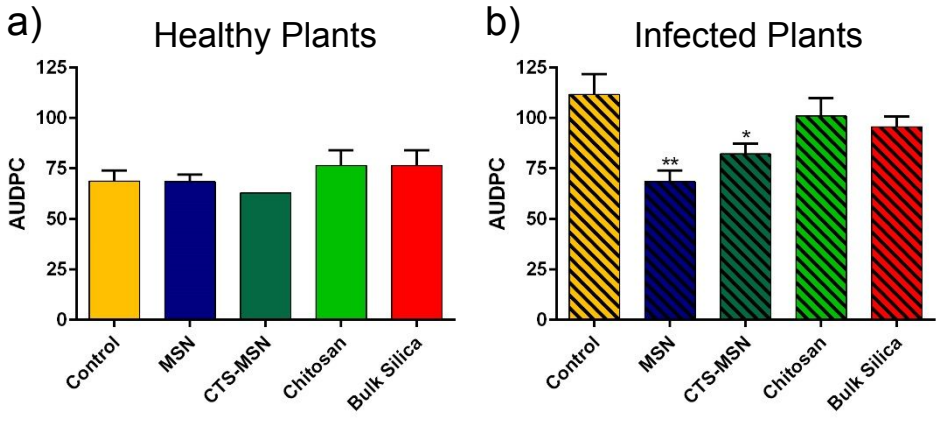


**Figure 4. In a) healthy plants, there is no difference in AUDPC following nanoparticle treatment; b) for *Fusarium*-infected watermelon, both MSNs and CTS-MSNs enhance disease suppression of *Fusarium* wilt. The error bars represent the standard error from six plants, with statistical significance testing done using a one-way ANOVA with Dunnett's multiple comparisons test to compare effects of the different treatments to the control. *p<0.05, **p<0.01**

**Gene Expression Changes**

The expression of several genes related to plant defense was investigated to gain a more fundamental understanding of the impact of the treatments (Figure 5). Notably, for many genes that are related to stress (CSD1, PAO, PPO, RAN1), treatment with MSNs, CTS-MSNs, or chitosan showed decreased expression. For PAO and PPO, reduced expression is also evident after treatment with bulk silica. The decreased expression in these genes suggests that the various treatments yielded some alleviation of the biotic stress of disease in these *Fusarium*-infected plants. This corroborates the reduced disease progress observed in the field after exposure of the plants to the nanoparticles. The findings for PPO and PR1 corroborate recent work in tomato plants treated with copper-based nanomaterials, which showed that expression of these genes was increased in early harvests, but that over time, the expression of these genes was reduced.[21] The expression of another stress-related gene, MDHA, was also reduced in plants that were treated with CTS-MSNs and chitosan. The similarity in expression after CTS-MSN and chitosan treatment suggests that the chitosan portion of CTS-MSNs is contributing to the stress-reducing mechanism. Interestingly, increased expression of MDHA is seen in bulk silica-treated plants, indicating greater stress from *Fusarium* wilt infection. There were no changes in CCH or COX11 expression (Figure S6); both of these are genes pertaining to maintenance of copper homeostasis and delivery of copper to cytochrome *c* oxidase complexes in the plant, respectively. There was also no change in expression of CYS (Figure S6), which is related to stress reduction in plants, but indirectly, as this gene encodes a compound that serves as a precursor for a different stress-related pathway. It is important to note that the expression of these genes was assessed at the end of the experiment. Since gene expression profiles of the plants can change based on age and life-cycle stage of the plant and on the time course of infection,[21] it is possible that the stress-related genes may have been differentially modulated earlier in the infection process for treated plants. However, by the end of the experiment when these measurements were taken,

the reduced disease burden on treated plants could lead to reduced expression of stress-related genes.

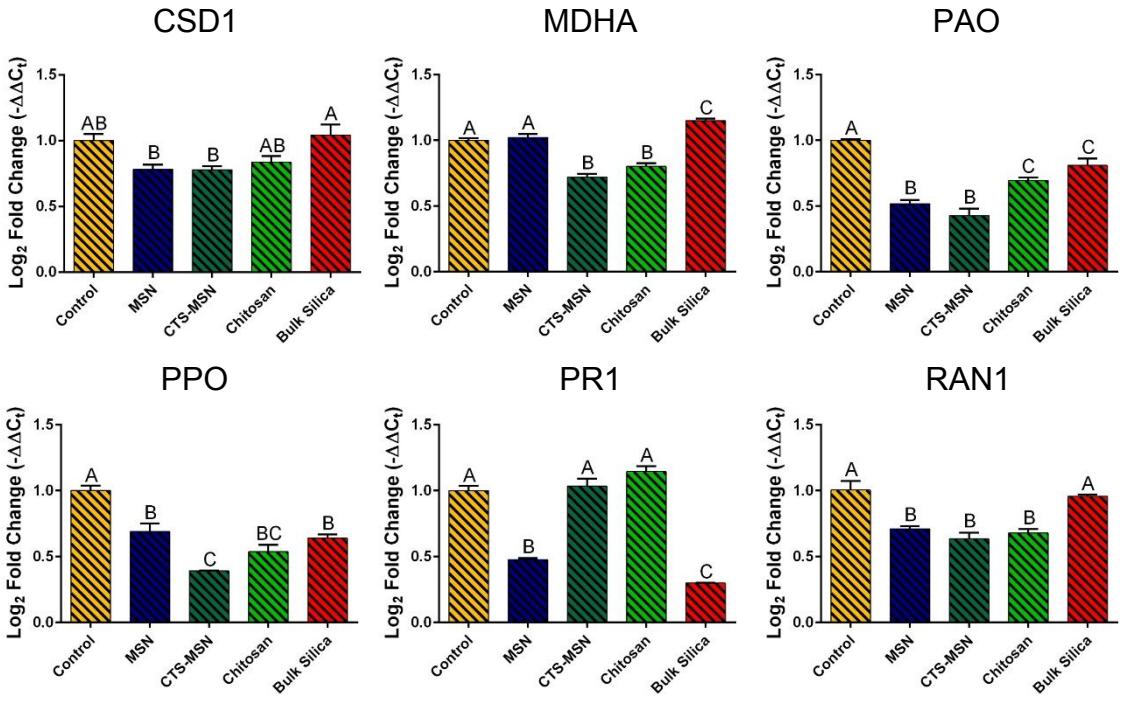


**Figure 5. Gene expression levels for CSD1, MDHA, PAO, PPO, PR1, and RAN1. The error bars represent the standard error from three replicates. Statistical significance was determined for each gene using a one-way ANOVA with Tukey's multiple comparisons test. Each sample with a different letter above indicates statistically significant differences with at least $p<0.05$.**

## Impact of Chitosan-coated MSNs on Fruit Yield

The fruit yield of watermelon under field conditions is an obviously critical endpoint for any nano-enabled strategy. Since disease reduction was observed for plants treated with MSNs and CTS-MSNs, it was hypothesized that these particles would improve the overall fruit yield. Fruits were harvested from plants 65 and 100 days post-planting, and the cumulative watermelon yield is shown (Figure 6). A single application of 1-2 mL of 500 mg/L CTS-MSNs to each healthy plant, via seedling dipping into the nanoparticle suspension, led to a 70% increase in watermelon yield, whereas none of the treatments applied to plants infected with *Fusarium* wilt caused any

appreciable change in fruit production. Since the number of fruits produced was relatively unchanged between treatments, this indicates that CTS-MSNs have significant potential for stimulating the yield of fruit under disease-free conditions. It is worth emphasizing that this increase in fruit yield was measured months after an initial treatment of the seedlings using a low amount of material (0.5-1 mg applied per plant). The lack of effect on plants grown with the pathogen in both locations is somewhat surprising given that the MSN treatments were effective in reducing disease severity in the greenhouse. We recognize that the supply of silicon to the plant occurred only at the seedling stage and that the yield enhancing effects were reduced. Multiple nanoparticle applications during growth may circumvent this obstacle. It is also possible that field variability and interaction of the pathogen with other stressors such as insects or minor pathogens could have overwhelmed any ameliorating effect of MSN treatment. Another factor may have been the excessive rainfall experienced in 2018, where the total rainfall for Connecticut during June, July, August, and September was twice the normal average and could have exacerbated the disease to the point where early life stage benefits of the MSNs were ineffective. Additional MSN applications during growth may be valuable as they would ensure a more continuous silicic acid supply and stimulate additional disease suppression. Such investigations are currently being planned.

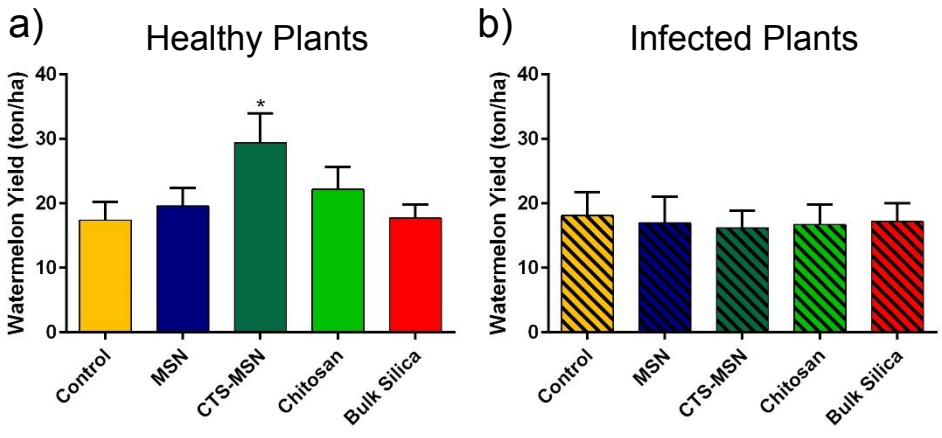


**Figure 6. When applied to a) pathogen-free watermelon plants that were grown at either of two locations (Griswold, CT or Hamden, CT), CTS-MSNs are showing a significant increase in the watermelon yield that is**

**not seen from any of the other treatments. For b) *Fusarium*-infected watermelon plants, no change in yield of fruit is seen for any of the nanoparticle treatments used. The error bars are from the standard error of twelve replicates. Statistical testing was performed with a one-way ANOVA with Dunnett's multiple comparisons test to compare the treatment effects to the control plants. *p<0.05**

### Changes in Biomass after NP exposure

Plant biomass was monitored in the greenhouse as another means of assessing the overall plant health in diseased and healthy conditions as a function of the treatments. Although the biomass measurements were statistically equivalent (Figure 7), the trends reflect the field findings where MSN and CTS-MSNs improve growth in the absence of the pathogen. The lack of significant differences is due to plant-to-plant variability. Similar trends were observed with the dry weights (data not shown). This result is somewhat surprising given the reduced disease progression by MSNs and CTS-MSNs seen above; however, given that the treatments were done when the plants were seedlings, differences in biomass may be masked after the several weeks of growth that had occurred by the time these measurements were taken. In other studies from our group using a range of plants and nanoparticle treatments,[21,22,40] reduced disease has been correlated with increased biomass; however, this correlation was not noted in all of these studies. The variability that has been observed is likely due to the use of a single application of nanoparticles, so that differences in response during subsequent growth and infections that can be observed weeks later are not surprising. This further suggests that use of multiple treatments over the growing period would be beneficial to maximize the benefits of the nanoparticles.

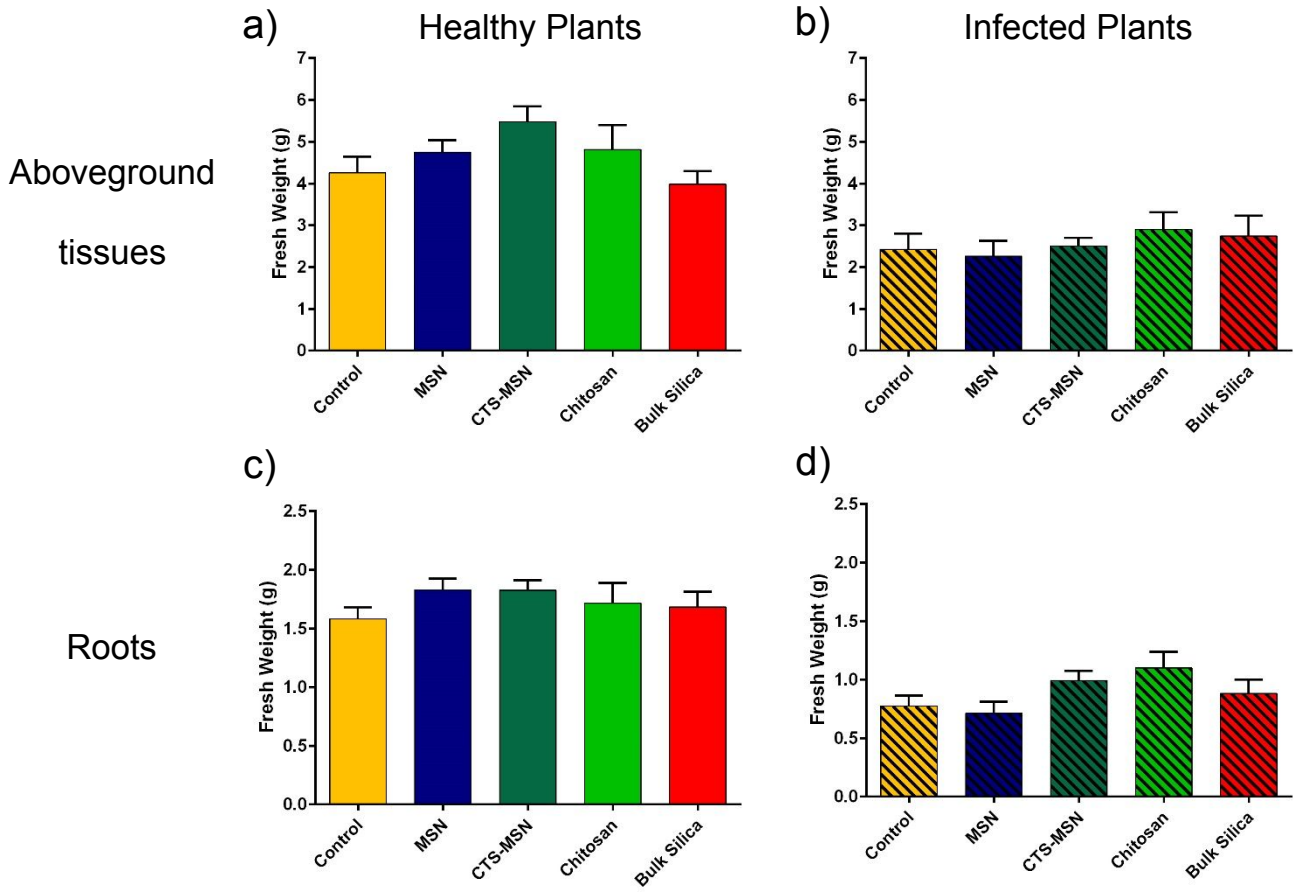


**Figure 7. The fresh weight of the aboveground tissues of a) healthy plants and b) *Fusarium*-infected plants; the roots of c) healthy watermelon plants and d) infected plants is unchanged regardless of the applied treatment. The error bars represent the standard error of ten replicate plants. A one-way ANOVA with Tukey's multiple comparisons test was used to evaluate statistical significance.**

## Silicon Content

At harvest, the silicon content of aboveground tissues, roots, and fruits were measured using ICP-MS (Figure 8). In all of the tissues tested, the silicon content in the treatment groups was not statistically distinct from that of the control plants. This is likely due the silicon being diluted during subsequent growth that followed after the young seedling was exposed to MSNs. That being said, there is a non-significant trend in the root data (Figure 8c) suggesting a slight increase in silicon incorporation in the roots of healthy *C. lanatus* after treatments. The lack of

increased silicon presence in the edible portions of the fruits is notable, as this indicates that the applied nanoparticles or the released silicic acid are not likely entering the edible tissues at any appreciable rate when compared to untreated controls. This may suggest there is minimal risk associated with the consumption of fruit from plants treated with silica nanoparticles. Eggplants exposed to nanoparticles of metal oxides similarly had no detectable increase in the respective metals[44] even though elevated amounts were present on the young treated plants.[45]

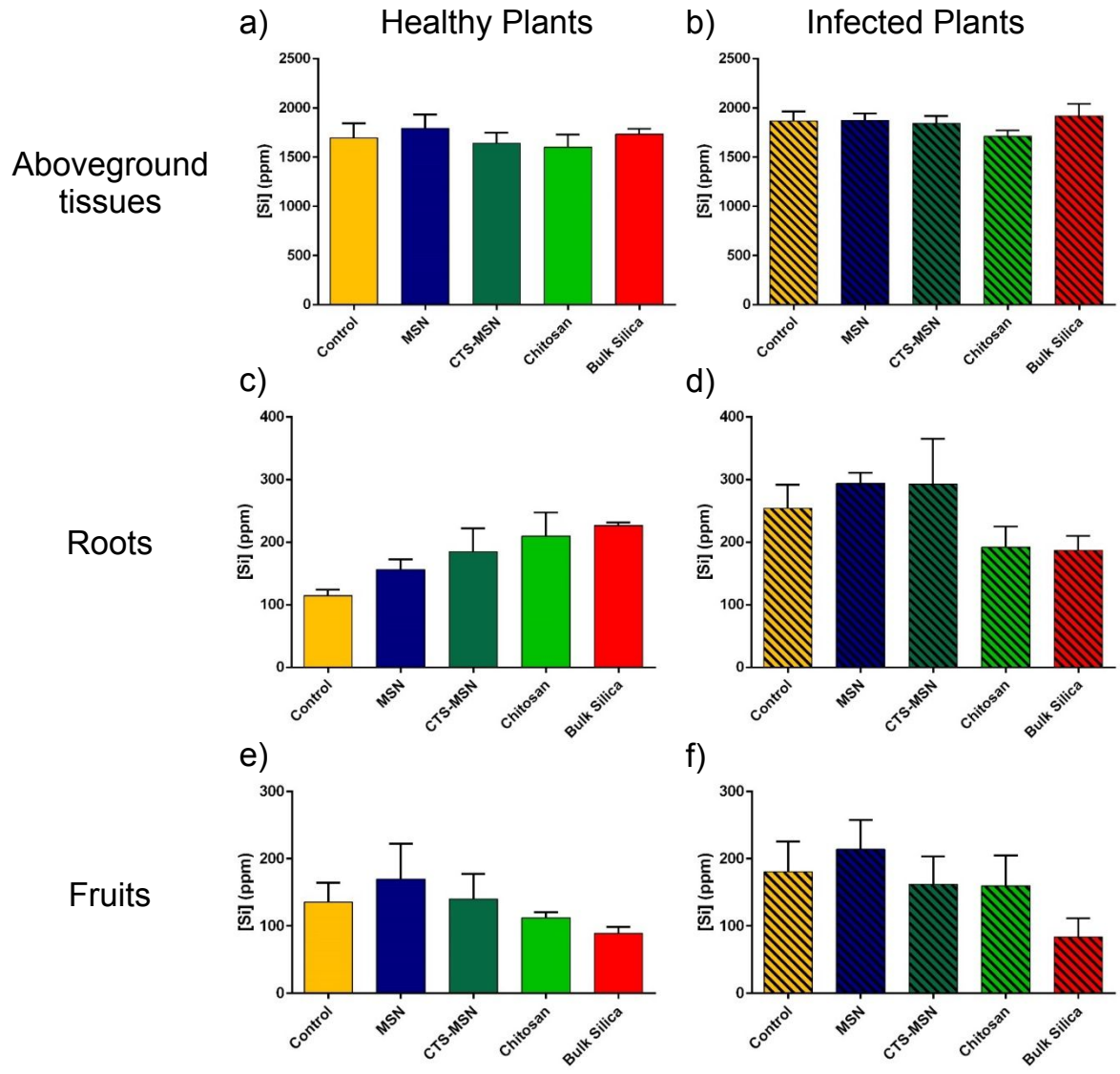


**Figure 8. The silicon content in the aboveground tissues of a) healthy plants and b) infected plants is unchanged by the nanoparticle application. The silicon content in the roots of c) healthy and d) *Fusarium*-infected *C. lanatus* is also unchanged. The edible portion of the fruits of watermelon plants has no appreciable**

**change in silicon content for e) healthy and f) infected plants. The error bars represent the standard error of five replicates. Statistical testing was performed using a one-way ANOVA with Tukey's multiple comparisons post hoc test.**

## Conclusions

Although the original motivation for this work was to investigate the effectiveness of dosing plants with MSNs and CTS-MSNs to improve disease resistance, the benefits of applying these materials to healthy plants was also evident. In fact, this is the first example where high surface area silica and chitosan were combined to enhance the health of crop plants. The approximately 70% increase in fruit yield from healthy plants after a single application of CTS-MSNs to seedlings prior to transplant demonstrates the utility of these materials to contribute to increased food production from plants, suggesting that there may be economic incentive to supplying watermelon plants with these particles. Furthermore, the increased germination of seeds that had been vacuum-infiltrated with CTS-MSNs is yet another indication that these nanoparticles have benefits to healthy plants. To plants that were infected with *Fusarium* wilt, a single application of MSNs or CTS-MSNs reduced disease progress, which was corroborated by gene expression data that showed reduced expression of stress genes in *C. lanatus*. Gene expression data also suggested that the presence of chitosan is contributing to the benefits of CTS-MSNs, as expression of stress-related genes was similar between plants that had been treated with CTS-MSNs and with chitosan alone. ICP-MS analysis of plant tissues did not reveal an accumulation of silica in the plants (due to growth dilution after initial exposure), and importantly, there was also no accumulation of silica in the edible tissues of the fruit, demonstrating that there should be minimal risk in their consumption. It is impressive that these benefits are observed in fully grown plants after a sub-milligram-dose was applied when the plants were young seedlings. Given the low dosage used in this work, the material cost of the CTS-MSN application was about $0.02/plant, or about $19/acre, making this a cost-efficient treatment method. To promote disease suppression and

plant growth even further in future work, the treatments will be applied to the seeds as well as the seedlings multiple times over the course of the growing period. Given that the plant treatments require only a small amount of material (0.5-1 mg per plant), multiple treatments still present a rather sustainable option for agricultural use. The sustainability is further enhanced by the high earth abundance of the precursor materials used. In addition, fluorescent mesoporous silica nanoparticles will be used to allow visualization of the NPs' location within the tissues as a means to further understand the observed agricultural benefits of these materials.

**Acknowledgements**

This work was supported by the National Science Foundation under the Center for Sustainable Nanotechnology, CHE-1503408. The CSN is part of the Centers for Chemical Innovation Program. J.T.B. acknowledges support by a National Science Foundation Graduate Research Fellowship (grant number 00039202). The authors gratefully acknowledge Dr. Marc A. Hillmyer for use of his thermogravimetric analyzer.

**ORCID IDs of Authors**

Joseph T. Buchman: 0000-0001-5827-8513

Wade H. Elmer: 0000-0003-3308-4899

Chuanxin Ma: 0000-0001-5125-7322

Kaitlin M. Landy: 0000-0002-8275-8469

Jason C. White: 0000-0001-5001-8143

Christy L. Haynes: 0000-0002-5420-5867

**Conflict of Interest**

The authors declare no competing financial interest.

## Supporting Information

Size distribution of MSNs; representative thermograms of MSNs and CTS-MSNs; infrared spectra of MSNs and CTS-MSNs; weather data for watermelon growing period; images of pathogen-free and *Fusarium*-infected plants; silicon content of vacuum-infiltrated seeds after loading with MSNs; expression of select genes after exposure

## References

(1) Savary, S.; Ficke, A.; Aubertot, J.-N.; Hollier, C. Crop Losses Due to Diseases and Their Implications for Global Food Production Losses and Food Security. *Food Secur.* **2012**, *4*, 519–537.

(2) Martyn, R. D. Fusarium Wilt of Watermelon: 120 Years of Research. In *Horticultural Reviews*; Janick, J., Ed.; John Wiley & Sons, Inc.: Hoboken, NJ, 2014; Vol. 42, pp 349–442.

(3) Lü, G.; Guo, S.; Zhang, H.; Geng, L.; Song, F.; Fei, Z.; Xu, Y. Transcriptional Profiling of Watermelon during Its Incompatible Interaction with *Fusarium oxysporum* f. sp. *niveum*. *Eur. J. Plant Pathol.* **2011**, *131*, 585–601.

(4) Zhang, Z.; Zhang, J.; Wang, Y.; Zheng, X. Molecular Detection of *Fusarium oxysporum* f. sp. *niveum* and *Mycosphaerella melonis* in Infected Plant Tissues and Soil. *FEMS Microbiol. Lett.* **2005**, *249*, 39–47.

(5) Zhang, M.; Xu, J. H.; Liu, G.; Yao, X. F.; Li, P. F.; Yang, X. P. Characterization of the Watermelon Seedling Infection Process by *Fusarium oxysporum* f. sp. *niveum*. *Plant Pathol.* **2015**, *64*, 1076–1084.

(6) Agricultural Marketing Resource Center, Products & Commodities: *Watermelon*; 2018. https://www.agmrc.org/commodities-products/vegetables/watermelon.

(7) Everts, K. L.; Himmelstein, J. C. Fusarium Wilt of Watermelon: Towards Sustainable

Management of a Re-Emerging Plant Disease. *Crop Prot.* **2015**, *73*, 93–99.

(8) Egel, D. S.; Hoke, S.; Cardinal, C. Evaluation of Triploid Watermelon for Resistance to Fusarium Wilt, 2010. *Plant Dis. Manag. Reports* **2010**, *3*, V135.

(9) Wu, H.-S.; Gao, Z.-Q.; Zhou, X.-D.; Shi, X.; Wang, M.-Y.; Shang, X.-X.; Liu, Y.-D.; Gu, D.-L.; Wang, W.-Z. Microbial Dynamics and Natural Remediation Patterns of *Fusarium*-infested Watermelon Soil under 3-yr of Continuous Fallow Condition. *Soil Use Manag.* **2013**, *29*, 220–229.

(10) Ren, L.; Su, S.; Yang, X.; Xu, Y.; Huang, Q.; Shen, Q. Intercropping with Aerobic Rice Suppressed *Fusarium* Wilt in Watermelon. *Soil Biol. Biochem.* **2008**, *40*, 834–844.

(11) Datnoff, L. E.; Rodrigues, F. Á.; Seebold, K. W. Silicon and Plant Disease. In *Mineral Nutrition and Plant Disease*; Datnoff, L. E., Elmer, W. H., Huber, D. M., Eds.; American Phytopathological Society: St. Paul, MN, 2007; pp 233–246.

(12) Bozarth, S. R. Diagnostic Opal Phytoliths from Rinds of Selected *Cucurbita* Species. *Am. Antiq.* **1987**, *52*, 607–615.

(13) Currie, H. A.; Perry, C. C. Silica in Plants: Biological, Biochemical and Chemical Studies. *Ann. Bot.* **2007**, *100*, 1383–1389.

(14) Wang, M.; Gao, L.; Dong, S.; Sun, Y.; Shen, Q.; Guo, S. Role of Silicon on Plant-Pathogen Interactions. *Front. Plant Sci.* **2017**, *8*, 701.

(15) Fawe, A.; Menzies, J. G.; Chérif, M.; Bélanger, R. R. Silicon and Disease Resistance in Dicotyledons. In *Silicon in Agriculture*; Datnoff, L. E., Snyder, G. H., Korndöfer, G. H., Eds.; Elsevier: Amsterdam, 2001; pp 159–170.

(16) Menzies, J.; Bowen, P.; Ehret, D.; Glass, A. D. M. Foliar Applications of Potassium Silicate Reduce Severity of Powdery Mildew on Cucumber, Muskmelon, and Zucchini Squash. *J. Am. Soc. Hortic. Sci.* **1992**, *117*, 902–905.

(17) Heine, G.; Tikum, G.; Horst, W. J. The Effect of Silicon on the Infection by and Spread of *Pythium aphanidermatum* in Single Roots of Tomato and Bitter Gourd. *J. Exp. Bot.* **2007**,

*58*, 569–577.

(18) Samuels, A. L.; Glass, A. D. M.; Ehret, D. L.; Menzies, J. G. Mobility and Deposition of Silicon in Cucumber Plants. *Plant, Cell Environ.* **1991**, *14*, 485–492.

(19) Khan, M. R.; Rizvi, T. F. Nanotechnology: Scope and Application in Plant Disease Management. *Plant Pathol. J.* **2014**, *13*, 214–231.

(20) Servin, A.; Elmer, W.; Mukherjee, A.; De la Torre-Roche, R.; Hamdi, H.; White, J. C.; Bindraban, P.; Dimkpa, C. A Review of the Use of Engineered Nanomaterials to Suppress Plant Disease and Enhance Crop Yield. *J. Nanoparticle Res.* **2015**, *17*, 92.

(21) Ma, C.; Borgatta, J.; Torre-Roche, R. D. La; Zuverza-Mena, N.; White, J. C.; Hamers, R. J.; Elmer, W. H. Time-Dependent Transcriptional Response of Tomato (*Solanum lycopersicum* L.) to Cu Nanoparticle Exposure upon Infection with *Fusarium oxysporum* f. sp. *lycopersici*. *ACS Sustain. Chem. Eng.* **2019**, *7*, 10064–10074.

(22) Borgatta, J.; Ma, C.; Hudson-Smith, N.; Elmer, W.; Pérez, C. D. P.; Torre-Roche, R. D. La; Zuverza-Mena, N.; Haynes, C. L.; White, J. C.; Hamers, R. J. Copper Based Nanomaterials Suppress Root Fungal Disease in Watermelon (*Citrullus lanatus*): Role of Particle Morphology, Composition and Dissolution Behavior. *ACS Sustain. Chem. Eng.* **2018**, *6*, 14847–14856.

(23) Kresge, C. T.; Leonowicz, M. E.; Roth, W. J.; Vartuli, J. C.; Beck, J. S. Ordered Mesoporous Molecular Sieves Synthesized by a Liquid-Crystal Template Mechanism. *Nature* **1992**, *359*, 710–712.

(24) Hussain, H. I.; Yi, Z.; Rookes, J. E.; Kong, L. X.; Cahill, D. M. Mesoporous Silica Nanoparticles as a Biomolecule Delivery Vehicle in Plants. *J. Nanoparticle Res.* **2013**, *15*, 1676.

(25) El Hassni, M.; El Hadrami, A.; Daayf, F.; Barka, E. A.; El Hadrami, I. Chitosan, Antifungal Product against *Fusarium oxysporum* f. sp. *albedinis* and Elicitor of Defence Reactions in Date Palm Roots. *Phytopathol. Mediterr.* **2004**, *43*, 195–204.

(26) Doares, S. H.; Syrovets, T.; Weiler, E. W.; Ryan, C. A. Oligogalacturonides and Chitosan Activate Plant Defensive Genes through the Octadecanoid Pathway. *Proc. Natl. Acad. Sci.* **1995**, *92*, 4095–4098.

(27) El Hadrami, A.; Adam, L. R.; El Hadrami, I.; Daayf, F. Chitosan in Plant Protection. *Mar. Drugs* **2010**, *8*, 968–987.

(28) Rabea, E. I.; Badawy, M. E.-T.; Stevens, C. V.; Smagghe, G.; Steurbaut, W. Chitosan as Antimicrobial Agent: Applications and Mode of Action. *Biomacromolecules* **2003**, *4*, 1457–1465.

(29) Bell, A. A.; Hubbard, J. C.; Liu, L.; Davis, R. M.; Subbarao, K. V. Effects of Chitin and Chitosan on the Incidence and Severity of Fusarium Yellows of Celery. *Plant Dis.* **1998**, *82*, 322–328.

(30) Bhaskara Reddy, M. V; Arul, J.; Angers, P.; Couture, L. Chitosan Treatment of Wheat Seeds Induces Resistance to *Fusarium graminearum* and Improves Seed Quality. *J. Agric. Food Chem.* **1999**, *47*, 1208–1216.

(31) Malerba, M.; Cerana, R. Recent Advances of Chitosan Applications in Plants. *Polymers (Basel).* **2018**, *10*, 118.

(32) Dzung, P. D.; Phu, D. Van; Du, B. D.; Ngoc, L. S.; Duy, N. N.; Hiet, H. D.; Nghia, D. H.; Thang, N. T.; Le, B. Van; Hien, N. Q. Effect of Foliar Application of Oligochitosan with Different Molecular Weight on Growth Promotion and Fruit Yield Enhancement of Chili Plant. *Plant Prod. Sci.* **2017**, *20*, 389–395.

(33) Mukta, J. A.; Rahman, M.; Sabir, A. A.; Gupta, D. R.; Surovy, M. Z.; Rahman, M.; Islam, M. T. Chitosan and Plant Probiotics Application Enhance Growth and Yield of Strawberry. *Biocatal. Agric. Biotechnol.* **2017**, *11*, 9–18.

(34) Nguyen, N. T.; Nguyen, D. H.; Pham, D. D.; Dang, V. P.; Nguyen, Q. H.; Hoang, D. Q. New Oligochitosan-Nanosilica Hybrid Materials: Preparation and Application on Chili Plants for Resistance to Anthracnose Disease and Growth Enhancement. *Polym. J.* **2017**, *49*, 861–

869.

(35) Yang, L.; Zhao, P.; Wang, L.; Filippus, I.; Meng, X. Synergistic Effect of Oligochitosan and Silicon on Inhibition of *Monilinia fructicola* Infections. *J. Sci. Food Agric.* **2010**, *90*, 630–634.

(36) Chen, J.; Wang, W.; Xu, Y.; Zhang, X. Slow-Release Formulation of a New Biological Pesticide, Pyoluteorin, with Mesoporous Silica. *J. Agric. Food Chem.* **2011**, *59*, 307–311.

(37) Lin, Y.-S.; Abadeer, N.; Hurley, K. R.; Haynes, C. L. Ultrastable, Redispersible, Small, and Highly Organomodified Mesoporous Silica Nanotherapeutics. *J. Am. Chem. Soc.* **2011**, *133*, 20444–20457.

(38) Chen, F.; Zhu, Y. Chitosan Enclosed Mesoporous Silica Nanoparticles as Drug Nano-Carriers: Sensitive Response to the Narrow pH Range. *Microporous Mesoporous Mater.* **2012**, *150*, 83–89.

(39) Schneider, C. A.; Rasband, W. S.; Eliceiri, K. W. NIH Image to ImageJ: 25 Years of Image Analysis. *Nat. Methods* **2012**, *9*, 671–675.

(40) Elmer, W.; De La Torre-Roche, R.; Pagano, L.; Majumdar, S.; Zuverza-Mena, N.; Dimkpa, C.; Gardea-Torresdey, J.; White, J. C. Effect of Metalloid and Metal Oxide Nanoparticles on Fusarium Wilt of Watermelon. *Plant Dis.* **2018**, *102*, 1394–1401.

(41) Jeger, M. J.; Viljanen-Rollinson, S. L. H. The Use of the Area under the Disease-Progress Curve (AUDPC) to Assess Quantitative Disease Resistance in Crop Cultivars. *Theor. Appl. Genet.* **2001**, *102*, 32–40.

(42) Karaman, D. Ş.; Sarwar, S.; Desai, D.; Björk, E. M.; Odén, M.; Chakrabarti, P.; Rosenholm, J. M.; Chakraborti, S. Shape Engineering Boosts Antibacterial Activity of Chitosan Coated Mesoporous Silica Nanoparticle Doped with Silver: A Mechanistic Investigation. *J. Mater. Chem. B* **2016**, *4*, 3292–3304.

(43) Benhamou, N.; Lafontaine, P. J.; Nicole, M. Induction of Systemic Resistance to Fusarium Crown and Root Rot in Tomato Plants by Seed Treatment with Chitosan. *Phytopathology*

**1994**, *84*, 1432–1444.

(44) Elmer, W. H.; Torre-Roche, R. D. La; Zuverza-Mena, N.; Dimkpa, C.; Gardea-Torresdey, J. L.; White, J. C. The Effect of Combinations of Nanoparticles of CuO, MnO, and ZnO on Yield and Verticillium Wilt of Eggplant. *Plant Dis.* **2019**, Submitted.

(45) Elmer, W. H.; White, J. C. The Use of Metallic Oxide Nanoparticles to Enhance Growth of Tomatoes and Eggplants in Disease Infested Soil or Soilless Medium. *Environ. Sci. Nano* **2016**, *3*, 1072–1079.

**For Table of Contents Only**

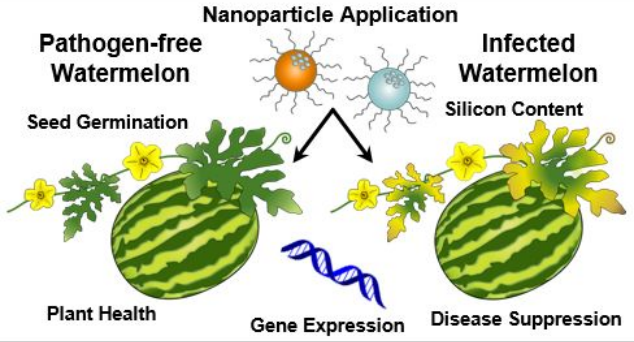


Synopsis:

Application of chitosan-coated mesoporous silica nanoparticles enhanced germination and fruit production in healthy watermelon and suppressed disease in infected plants.